A study on the performance and emissions of HCCI oxy-fuel combustion in a CFR engine with recirculated carbon dioxide

Author, co-author (**Do NOT enter this information. It will be pulled from participant tab in MyTechZone**)

Affiliation (Do NOT enter this information. It will be pulled from participant tab in MyTechZone)

Abstract

Stringent emission regulations and the anticipated climate change call for a paradigm shift in the design of the conventional internal combustion engines. One way to combat this problem is oxy-fuel combustion in which the combustion products are mainly water vapor and carbon dioxide. Water vapor can be easily separated by condensation and carbon dioxide is then easily captured and stored. However, many technical challenges are associated with this mode of combustion. There are many challenges facing oxy-fuel combustion before it find its way to commercial production especially for internal combustion engines. One such challenge is the relatively high temperature of the oxy-fuel combustion. A solution to this problem is the recirculation of the generated CO_2 to moderate the in-cylinder temperature. Therefore, careful study of the effect of recirculating the CO_2 back to combustion chamber is needed before the implementation of such a concept. This study is a continuation of a previous work published by the authors. In the previous study, the performance and emissions of an oxy-fuel HCCI engine were investigated. The in-cylinder temperature was moderated by supplying the engine with fresh CO_2 from gas cylinders.

In this present work the performance of the same oxy-fuel HCCI engine is investigated but the difference is that the in-cylinder temperature is regulated by recirculating the generated CO_2. The experiments were conducted in a variable compression CFR engine that was modified to operate in oxy-fuel mode with recycled carbon dioxide. The emissions were also measured using an FTIR exhaust analyzer. The results showed that the implementation of this concept is possible. However, the indicated thermal efficiency deteriorates due to lower combustion and gas exchange efficiencies. Also, the CO_2 recirculation resulted in higher CO and unburned hydrocarbon (UHC) emissions.

Introduction

The data and scientific theories explaining climate change have been subjected to rigorous scientific peer reviewing making the sources of information on climate change impeccable [1,2]. In 2017, the U.S. Global Change Research Program (USGCRP) expressed 90% confidence that climate change is a direct result of the greenhouse gas (GHG) emissions from fossil fuels [3]. Almost 10% of those emissions are emitted by internal combustion engines (ICEs) [4] and this calls for effective solutions to either improve the existing engines or even replace them with novel alternatives. The ICE community is responding by accelerating research and development activities to effectively reduce the CO_2 footprint of the combustion engines [5]. The advances in engine research include, but are not limited to, improving fuel economy, assessing the feasibility of unconventional fuels, and electrification [5,6].

In a cradle-to-grave analysis, Algowainy et al. [7] showed that a combination of engine technologies and renewable fuels could decrease the greenhouse gas emissions by 10-30% of their current amounts. Homogenous charge compression ignition (HCCI) engines are one of those technologies that could push the boundaries of the ICE efficiency [8]. HCCI is a lean burn strategy in which a homogenous charge of fuel and oxidizer is premixed and then compressed until auto-ignition occurs. HCCI combustion is associated with high efficiency due to several reasons. The lean equivalence ratio and low temperature increase the specific heat ratio and hence the thermodynamic efficiency. The low temperature decreases the heat transfer losses as well. Also, the auto-ignition requires higher compression ratios that give higher thermodynamic efficiency. One more reason for improved efficiency is the less pumping work because the engine is typically not throttled. The low temperature also decreases the harmful thermal NOx emissions. Despite these advantages, the HCCI engine did not find its way to industry because of its limited operating range and relatively fast combustion. Being dependent on the auto-ignition of a premixed charge, lower loads could cause misfires while higher loads may lead to lethal knock events [9]. The relatively fast combustion is another challenge that can be tackled by many techniques such as mixture dilution and fast thermal management [10].

Aside from enhancing engine efficiency, the combustion of unconventional fuels could reduce the CO_2 emissions just equally. For example, combustion of hydrogen and ammonia does not have any carbon footprint but there are also many practical and environmental challenges associated with the deployment of such low carbon fuels. Electrification is another promising technology that could reduce the vehicle CO_2 emissions [11]. Notwithstanding its importance, the effectiveness of electrification to reduce CO_2 emissions is sometimes overestimated. Given the fact that battery production is not a CO_2 free process, an ICE vehicle may emit less carbon dioxide than a BEV if a comprehensive life cycle assessment is conducted [12].

Oxy-fuel combustion is one of the best ways to eliminate CO_2 emissions [13]. The fuel is burned with pure oxygen as the oxidant instead of air. Consequently, NOx emissions are eliminated and the combustion products are mainly CO_2 and H_2O. Water can be separated conveniently by condensation while some of the generated CO_2 can be recycled to moderate the combustion

10/19/2016

temperature and the rest can be sequestrated and stored for subsequent utilization. Recycling some of the generated CO_2 is necessary to reduce the high adiabatic flame temperature of oxy-fuel combustion. On the one hand, the advantage of oxy-fuel combustion is the convenience of CO_2 capture and storage, but on the other hand, oxy-fuel combustion requires more complex and costly systems for oxygen separation. In fact, one of the hurdles facing the implementation of oxy-fuel combustion in vehicle engines is the oxygen separation. It is strenuous to have an on-board oxygen separator unit but some researchers suggest that the vehicle can carry its own oxygen supply and store the captured CO_2 [14]. This will require changes in the infrastructure of the fuel stations because the vehicle will need to simultaneously refuel, dispose the captured CO_2, and replenish the oxygen supply. Advancements in membrane technology for oxygen separation could also make the on-board oxygen separation a reality. But some challenges regarding the thermal and chemical stability of the membrane have to be addressed before it finds its way to industrial production [15].

Oxy-fuel combustion in internal combustion engines is not a new concept. It dates back to the 1920s when hydrogen-oxygen combustion was investigated in connection with submarine propulsion [16]. Recently, this concept has been revisited as one of the best ways to eliminate CO_2 emissions [17]. Wu et al. studied oxy-fuel combustion in SI engines with water injection to moderate the in-cylinder temperature [18]. They showed that utilizing exhaust energy to preheat the injected water results in better efficiency. This concept of preheating the injected water by recovering some of the waste heat in oxy-fuel internal combustion engines is known as internal combustion Rankine cycle (ICRC). Better emissions of the ICRC engines have been also reported beside their improved efficiency [19]. It has been shown that the economic feasibility of the ICRC concept for automobiles could be superior to those based on fuel cells and biofuels [14]. However, water injection has its undesirable side effects such as corrosion and wear due to poor lubrication [20]. Diesel-like compression ignition oxy-hydrogen combustion has been simulated by Boretti et. al [21]. They concluded that the main challenge facing this novel engine is the unacceptably high in-cylinder temperature and they suggested recirculating the generated steam to reduce that temperature. Oxy-fuel combustion based on auto-ignition of a premixed charge has been slightly studied with the lack of exhaustive experimental approaches. Simulations conducted for auto-ignition in a 2-stroke engine revealed its potential for better efficiency and emissions [22].

The combustion of carbon fuels and the recirculation of the generated CO_2 can efficiently mitigate the problem of the oxy-fuel high in-cylinder temperature. Due to its high specific heat, CO_2 can absorb the released heat and keep the temperature at reasonable limits. Oxygen and carbon dioxide systems have been implemented in test benches to simulate the adoption of exhaust gas recirculation but no actual recirculation was made [23,24]. The results showed that CO_2 decreases the in-cylinder temperature significantly and prolonged combustion durations are perceived.

This paper is a follow up on a previous study published by the authors [24]. The previous paper studied the HCCI combustion of n-heptane with both air and an oxygen/CO_2 mixture as oxidants but without recirculation. In the present study, the results from the previous paper were repeated at different conditions but also a third case was introduced. n-heptane was now combusted with a mixture of oxygen fed to the engine and CO_2 recycled from the exhaust. The main question is whether there is a difference between fresh CO_2 from gas cylinders and CO_2 recycled from the exhaust, i.e. dry EGR. The dry EGR will contain not only CO_2 but rather concentrations of unburned hydrocarbons, carbon monoxide, and perhaps some traces of NOx and other impurities. Many studies on the effect of various components such as NOx, N_2O_2, HC, and CO

have been conducted on HCCI engines. To the best of the authors' knowledge, this is the first work to study a mixture of oxygen and fresh CO_2 from gas cylinders and compare it to pure oxygen and recirculated CO_2 in HCCI engines.

Experimental Setup

The experiments were conducted on a cooperative fuel research (CFR) engine. It is a variable compression ratio engine that has been used for decades to measure the octane numbers of the internal combustion engine fuels [25]. The CFR engine is designed for SI combustion close to stoichiometry but the design has been modified to adapt to the lean conditions of the present study. The changes included replacing the carburetor with a port fuel injector for enhanced equivalence ratio (ϕ) control. ϕ was controlled by supplying the fuel at constant pressure of 4 bar and tuning the injection duration to attain the required ϕ. The equivalence ratio ϕ was measured by measuring the flows of both the oxidizers and fuels using mass flow controllers. Table 1 summarizes the specifications of the CFR engine used in the experiments.

Table 1. CFR engine specifications

Parameter	Value	Unit
Displaced volume	611.7	cc
Stroke	114.3	mm
Bore	82.55	mm
Connecting rod	256	mm
Compression ratio R_c	Variable (4 to 18)	-
Number of valves	2	-
Exhaust valve opening	140	CAD aTDC
Exhaust valve closure	-345	CAD aTDC
Inlet valve opening	-350	CAD aTDC
Inlet valve closure	-146	CAD aTDC
Coolant water temperature	100 ± 1.5	ºC
Oil temperature	57 ± 8	ºC

The intake and exhaust pressures were measured using water-cooled *AVL* pressure transducers. The in-cylinder pressure was measured using an *AVL QC34D* pressure transducer. The crank angle encoder registers a pressure measurement at each 0.2 CAD. Thermocouples were installed to monitor the temperatures of the intake, exhaust, coolant water, and oil. The different gas flows were controlled using a *Brooks* mass flow controller (MFC) for each gas stream. Combustion emissions were also measured by an *AVL SESAM i60* FTIR analyzer to estimate the combustion efficiency and compare the emissions per se. The exhaust oxygen concentration was measured using a *Bosch LSU ADV* sensor. It should also be noted that 200 cycles were measured for each operating point and all the measurements were repeated three times to ensure data repeatability. The heat release rate was individually evaluated for each cycle (without any filtration) and then the 200 cycles were averaged to give a mean HRR. The mean HRR was then filtered using the 1-D digital filter function in MATLAB.

Table 2 summarizes the accuracy of the different devices used in the experiment.

Table 2. The accuracy of the different devices used in the experiment

Device/System	Accuracy
Intake and exhaust pressure transducers	± 0.1% of the full scale (10 bar)
QC34D AVL pressure transducer	± 0.3% of the full scale (150 bar)
Thermocouples	± 2 K
Mass flow controllers (MFCs)	± 0.5 % of the flow rate and ± 0.1 % of the full scale (1000 slpm)
FTIR analyzer	≤ 2% of the measured value
Bosch LSU ADV sensor	≤ 5% of the measured value

As mentioned in the introduction, three different cases were studied and compared in this paper. The first case is normal combustion with dry air as the oxidizer. The second and third cases are the oxy-fuel combustion cases but the difference between them is that the exhaust of the latter is recirculated back to the intake after combustion via an EGR valve. Table 3 shows the compositions of the three different oxidizer mixtures at the intake. Case 1 represents the standard dry air composition and its flow was controlled by a mass flow controller. In case 2, fresh CO_2 gas acts as a thermal buffer and it was supplied with O_2 to reduce the adiabatic flame temperature of the oxy-fuel combustion. The flow rates of both CO_2 and O_2 were also controlled using mass flow controllers.

Case 3 needs more explanation as it is the main objective of these experiments. At the beginning, both fresh O_2 and CO_2 are supplied to the engine. If only O_2 is supplied, the adiabatic flame temperature will be very high and it may cause detrimental knock. The exhaust in this case will be composed of 6 different components: CO_2 supplied from gas cylinders, CO_2 and H_2O produced during combustion, the remaining O_2 because of the HCCI lean condition, and finally negligible amounts of other emissions such as CO and unburned hydrocarbons (UHC). An exhaust back pressure valve is used to increase the exhaust pressure and drive the exhaust gases through an EGR valve. The recirculated exhaust gases are then passed through a plate and frame heat exchanger to separate water by condensation. The back pressure valve was controlled to have the exhaust pressure at 1.5 bar since the pressure loss through the EGR valve and the heat exchanger is less than 0.5 bar (the intake pressure was kept at 1 bar i.e. the flow will always be from the exhaust to the intake). The flow of fresh CO_2 is then decreased gradually until enough CO_2 is accumulated and equilibrium is achieved. For case 3, The flow of fresh O_2 to the intake was kept constant by a mass flow controller. A *Bosch LSU ADV* sensor was used to measure the proportion of the leftover oxygen in exhaust gases, i.e. the recirculated O_2. Knowing the oxygen concentration the rest should be mainly the recirculated CO2 to keep the intake temperature at 1 bar. Table 3 shows the intake composition at equilibrium for the three different cases.

Table 3. The equilibrium intake composition for the three different mixtures

Case	1	2	3
Oxidizer mixture	Air	CO_2+O_2	CO_2+O_2 (Recirculated)
Fresh O_2 (%vol.)	20.95	21.0	9.2
Recirculated O_2 (%vol.)	0	0	11.8
N_2 (%vol.)	78.09	0	0
Ar (%vol.)	0.93	0	0
Fresh CO_2 (%vol.)	0	79.0	0
Recirculated CO_2 (%vol.)	0	0	79.0

The intake pressure was kept constant at 1 bar with an intake temperature of 149 ºC for all the three cases. The intake temperature is relatively high since carbon dioxide absorbs the released heat and decreases the in-cylinder temperature and to account for this cooling effect the intake temperature has to be increased. It is worth mentioning that the intake temperature of 149 ºC corresponds to the temperature of the motor octane number (MON) testing method [26]. HCCI is lean combustion with a limited equivalence ratio (ϕ) range. An equivalence ratio lower than this range may result in poor combustion stability and misfires while higher equivalence ratios can cause severe knock and lethal damage to the engine. It was decided to run the engine at an equivalence ratio of 0.4 to enhance the combustion stability and avoid any misfires or severe knock events. Finally, the fuel used for all experiments is n-heptane which is the zero reference for the RON and MON scales. N-heptane's high reactivity is especially useful given that we are dealing with CO_2, which has a low specific heat ratio that decreases the in-cylinder temperature which might otherwise stunt the combustion process. Tables 4 and 5 summarize the testing conditions and the n-heptane properties, respectively.

Table 4. Experimental testing conditions

Parameter	Value	Unit
Rotation speed	600	rpm
Intake temperature	149	ºC
Intake pressure	1	bar
Equivalence ratio ϕ (Fuel/Oxygen)	≈ 0.4	-
Fuel	n-heptane	-

Table 5. n-heptane properties

Property	Value	Unit
RON	0	-
MON	0	-
Auto-ignition temperature	493	K
Boiling point	371	K
Molecular formula	C_7H_{16}/ $CH_3(CH_2)_5CH_3$	-
Molar mass	100.23	g/mol
Density (at 20ºC)	679.5	kg/m^3

Finally, it should be emphasized that CA50 is the crank angle at which 50% of heat is already released. Since the compression ratio can be easily varied in a CFR engine, it was decided to phase the combustion by changing the compression ratio. Increasing the compression ratio results in advancing CA50 and vice versa. This is discussed more in the *results and discussion* section of this paper. Figure 1 shows a general schematic for the experimental setup.
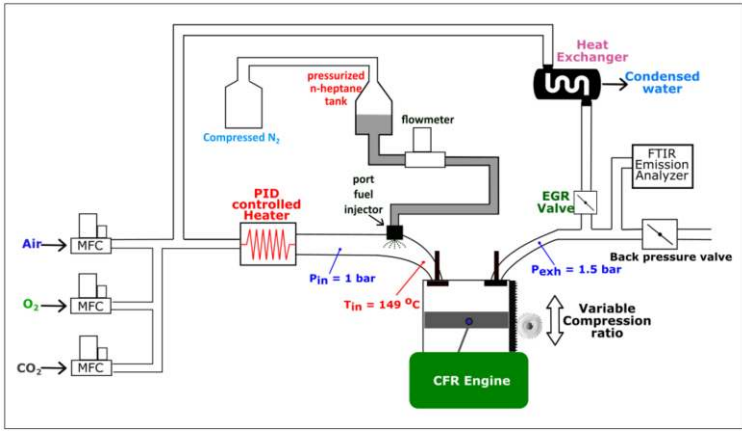
Figure 1. Experimental Setup schematic

Results and discussion

The results first show the in-cylinder pressure for the three different mixtures. The temperature profile is then inferred from the pressure trace which is used later to estimate the specific heat ratio. The heat release analysis is then shown and discussed. This section finally concludes with the emission results and the efficiency analysis.

In-cylinder pressure and temperature

As previously mentioned combustion was phased to have CA50 at TDC for all the three cases. The compression ratio required to have CA50 at TDC is not the same for the three cases because each mixture has different specific heat ratio (γ). Table 6 shows the required compression ratio (R_C) to have CA50 at TDC for each case.

Table 6. Required compression ratio (R_c) to have CA50 at TDC for each case

Case	Oxidizer mixture	R_c for CA50
1	Air	7.2
2	CO_2+O_2	17.1
3	CO_2+O_2 (Recirculated)	16.9

Figure 2 shows the pressure traces for the three different cases. It can be noticed that the CO_2 mixtures required higher compression ratio to have the CA50 at TDC. Also, the recirculation of the cooled exhaust gases does not show obvious differences from the uncirculated case. It might be useful to also mention that the in-cylinder pressure shown in figure 2 was measured using a piezoelectric transducer that gives a relative pressure. A process called pegging refers this relative pressure to a known pressure. In this study the piezoelectric signal was pegged by assuming that the in-cylinder pressure is equal to the intake pressure at IVC.
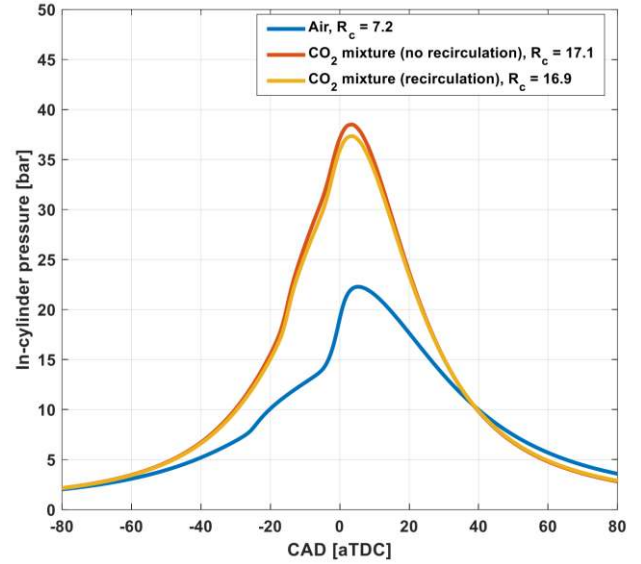

Figure 2. In-cylinder pressure for the three different mixtures

If ideal gas behavior is assumed then the observed trends in figure 2 can be explained in light of the isentropic relations in which the pressure and temperature evolution depend on the specific heat ratio of the mixture as in equations 1 and 2.

$$P_2 = P_1 R_c^{\gamma} \qquad (1)$$
$$T_2 = T_1 R_c^{\gamma-1} \qquad (2)$$

Where
P is the in-cylinder pressure
T is the in-cylinder temperature
R_c is the compression ratio
γ is the specific heat ratio

The specific heat ratio γ of an ideal gas can be expressed in terms of the degrees of freedom as follows:

$$\gamma = 1 + \frac{2}{f} \qquad (3)$$

Where
f is the degrees of freedom of the gas

This means that, for any gas, the specific heat ratio is greater than 1 and, at the same time, smaller than 2 since the minimum possible degrees of freedom is 3 representing the three translational movements of a monoatomic molecule. Coming back to equations 1 and 2 it can be noticed that the pressure evolves with compression ratio (R_c) raised to an exponent greater than 1 while the temperature evolves with R_c raised to an exponent less than 1. This implies that the pressure will evolve much faster than the temperature in general. Also, equation 3 implies that the specific heat ratio of a gas decreases when its temperature increases since it will gain more degrees of freedom.

For the gas mixtures presented in this study, the specific heat ratio for each mixture can be estimated by a model utilizing Burcat's thermodynamic data [27]. The model assumes 100% reactants before TDC and 100% complete combustion products after TDC. Of course this is not an accurate estimation but it helps in the understanding of the results. Figure 3 shows the results of the specific heat ratio model.
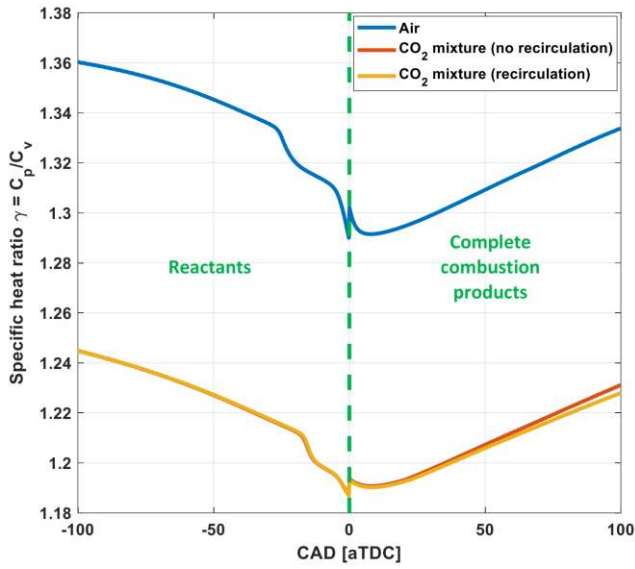
10/19/2016

Figure 3. Specific heat ratio γ as a function of the crank angle

As expected CO_2 mixtures have less specific heat ratio since CO_2 possesses higher degrees of freedom. It can be noticed that the specific heat ratio decreases as the in-cylinder temperature increases reaching its minimum at TDC. The abrupt change in the specific heat ratio at TDC is a direct result of the crude estimate that the gas mixture consists of 100% reactants before TDC and 100% complete combustion products after TDC.

Chemical kinetics control HCCI combustion and temperature plays a vital role in the initiation of the reactions. While the in-cylinder pressure is measured, the in-cylinder temperature is not and it has to be calculated from the known pressure trace. The average in-cylinder temperature can be calculated as a function of the crank angle position as follows:

$$T(CAD) = \frac{P(CAD)\,V(CAD)\,n(CAD)}{P_{ivc}\,V_{ivc}\,n_{ivc}}\,T_{ivc} \qquad (4)$$

Where n is the moles of the gas inside the cylinder and the subscript ivc stands for the intake valve closing.

All the variables on the right side of equation 4 are known except T_{ivc} which needs to be approximated. One way to estimate T_{ivc} is to use the ideal gas equation as follows:

$$T_{ivc} = \frac{1}{\left(n_o + n_f + n_{res}\right)} \times \frac{P_{ivc}V_{ivc}}{R} \qquad (5)$$

P_{ivc} is measured, V_{ivc} is known from the engine geometry, n_o is the moles of the oxidizer whether it is air or O_2/CO_2 mixture, and n_f is the moles of fuel. The moles of the residuals n_{res} can be found using the ideal gas equation at exhaust valve closing: $n_{res} = \frac{P_{evc}V_{evc}}{R\,T_{evc}}$. The problem here is that the temperature at exhaust valve closing T_{evc} is not known but it has been proven experimentally that the moles of the residual gases can be estimated with a good accuracy if the exhaust pressure and temperature are used in the previous formula [28]. Thus, n_{res} is estimated as:

$$n_{res,estimate} = \frac{P_{exh}V_{evc}}{R\,T_{exh}} \qquad (6)$$

The in-cylinder temperature can then be calculated with a fair accuracy. Figure 4 shows the in-cylinder temperature as a function of the crank angle degree. It is clear from the figure that the initiation of the exothermic reactions happens at the same

temperature of approximately 700 K for all the three different mixtures. This was the reason for increasing the compression ratio in the case of the CO_2 mixtures. It was simply to attain the required temperature for n-heptane auto-ignition. It is worth mentioning that the in-cylinder temperature was estimated from the pressure trace using ideal gas equation.
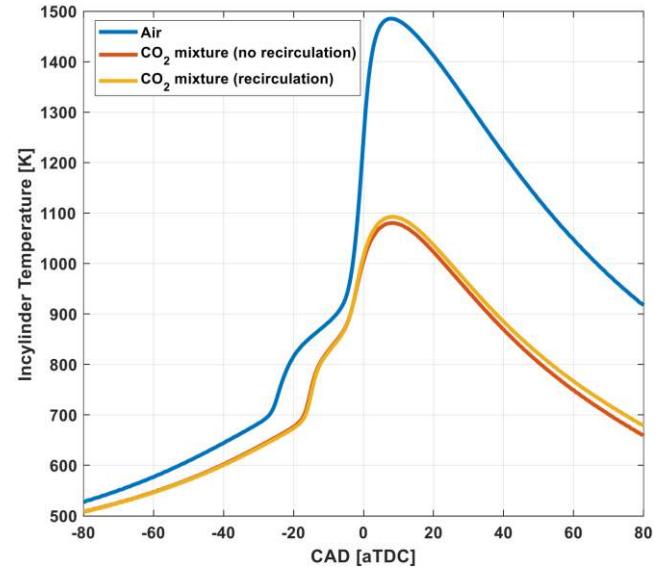

Figure 4. In-cylinder temperature for the three different mixtures

From figure 4 it can be seen that the increase in temperature after the initiation of the reactions is higher for the air mixture. This behavior is explained in light of equation 7.

$$\Delta T = \frac{Q}{N c_v} \qquad (7)$$

Where
ΔT is the change in gas temperature
Q is the energy added to the system
N is the number of moles of the charge
c_v is the molar based constant volume specific heat

The CO_2 mixtures have lower combustion efficiency η_c as shown later in this paper. This means lower energy added to the system and hence lower temperature increase for the CO_2 mixtures. Furthermore, the CO_2 mixture has higher specific heat, hence lower temperature increase is expected.

Two rise events can be observed in each pressure and temperature trace implying the existence of two distinct heat release phases. The reasons behind these phases will be discussed in more details. Finally, it can be noticed from figures 2-4 that the recirculation of CO_2 does not affect the oxy-fuel combustion significantly. However, a slightly lower compression ratio is needed for the recirculated case which is a direct result of the accumulation of CO and UHC that enhances the autoignition as will be seen later in the emission analysis.
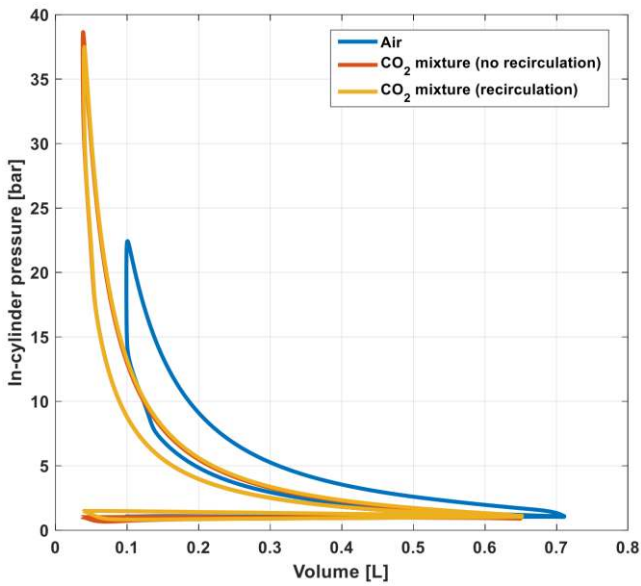
Pressure-Volume diagram

Figure 5. P-V diagrams for the three different mixtures

Figure 5 shows the P-V diagram for the three different mixtures. It gives useful information when two parts of the graph are magnified. The first part is the gas exchange area shown in figure 6.
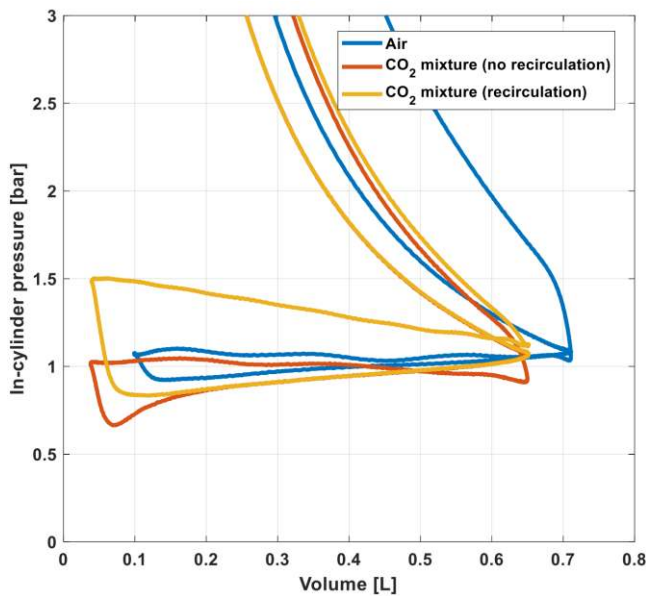

Figure 6. Magnified version of figure 5 to highlight the gas exchange part of the cycle

In the case of the recirculated CO_2 mixture, the exhaust pressure should be always greater than the intake pressure to drive the EGR in the right direction. This was achieved by a back pressure valve as discussed earlier in the experimental setup. For this reason the recirculated CO_2 mixture has the maximum exhaust pressure which results in higher pumping losses and consequently poor gas exchange efficiency. This can be seen in figure 6 where the gas exchange area for the recirculated CO_2 mixture is the largest. The efficiency analysis presented later in this paper will shed light on the gas exchange efficiency and its importance.

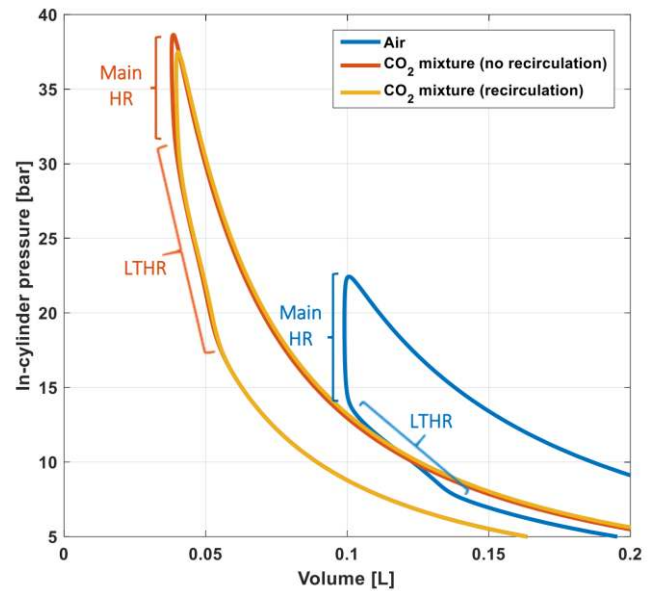The second part of interest in the *P-V* diagram is the heat addition area as shown in figure 7.

Figure 7. Magnified version of figure 5 to highlight the heat addition part of the cycle

It is clear from figure 7 that the heat addition happens at two consecutive stages which are low temperature heat release (LTHR) followed by the main heat release. Using n-heptane as a fuel in these experiments is the reason behind these stages. n-heptane is the zero reference for the RON scale and its combustion is associated with prominent (LTHR) as found by Singh et al. [29].

Heat release rate (HRR)

Using the first law of thermodynamics and by assuming ideal gas behavior, the heat release rate in the combustion chamber is given as follows [30]:

$$\frac{dQ_{hr}}{d\theta} = \frac{\gamma}{\gamma - 1} p \frac{dV}{d\theta} + \frac{1}{\gamma - 1} V \frac{dp}{d\theta} + \frac{dQ_{ht}}{d\theta} \qquad (8)$$

Where

$\frac{dQ_{hr}}{d\theta}$ is the heat release rate (HRR) per crank angle degree (CAD)

γ is the specific heat ratio $\frac{c_p}{c_V}$

p is the in-cylinder pressure

V is the volume of the cylinder

$\frac{dV}{d\theta}$ is the rate of volume change per crank angle degree

$\frac{dp}{d\theta}$ is the rate of pressure change per crank angle degree

$\frac{dQ_{ht}}{d\theta}$ is the rate of heat transfer losses per crank angle degree

The model shown in equation 8 accounts for the heat transfer losses estimated using Woschni's correlation [31]. Other losses such as blow-by and crevice losses are neglected in this study. Figure 8 shows the heat release rate for the three different cases.
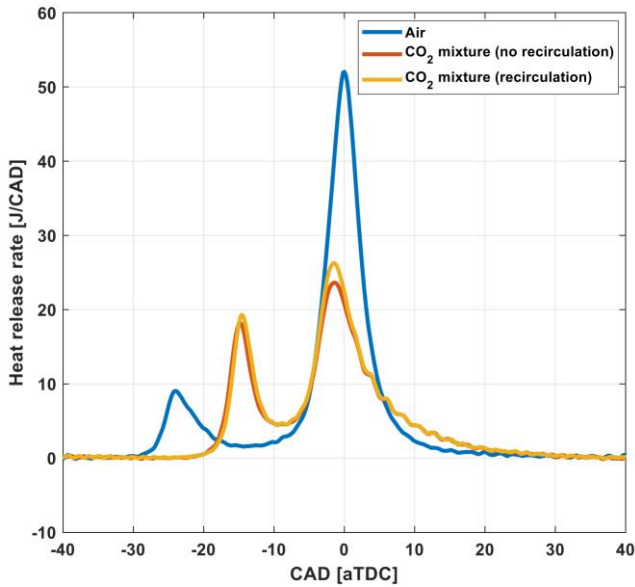
Figure 8. Heat release rate for the three different mixtures

Figure 9. Accumulated heat release for the three different mixture

As demonstrated earlier, the left and right peaks associated with each case correspond to the LTHR and main HR, respectively. LTHR appears during the combustion of reactive fuels in internal combustion engines [29]. Low engine speed is another reason for the LTHR since it gives the low temperature reactions sufficient residence time to develop [29]. Also, it is clear that the recirculation of the CO_2 has little or no effect on the heat release rates.

Another observation in figure 8 is that the rate of the main HR of the CO_2 mixtures is slower than the air mixture due to both the thermal and chemical effects of CO_2. The thermal effect is related to the high heat capacity of CO_2 that enables the mixture to absorb the released heat without a significant temperature increase. The low temperature means slower chemical kinetics and hence slower rates of heat release. The high heat capacity of CO_2 is not the only reason for slowing the system reactivity. The chemical effect related to the possibility of CO_2 to directly participate in chemical reactions is also another reason. CO_2 enhances the methyl recombination reactions because its third body efficiency is three times higher than that of N_2. For the considered temperatures ($900\,K < T < 1100\,K$), the methyl recombination reactions becomes faster than the methyl oxidation reactions and system reactivity slows down [32]. The rate of low temperature heat release (LTHR) shows the opposite behavior, i.e. LTHR is higher for the CO_2 mixtures. At low temperature, CO_2 increases the system reactivity by accelerating an OH formation pathway $H_2O_2 + M = OH + OH + M$ but once the temperature increases the methyl recombination reactions dominate and the system reactivity slows down [32]. In short, CO_2 increases the system reactivity at low temperatures and decreases the reactivity at high temperatures. Also, a slightly higher heat release rate is noticed for the recirculated CO_2 mixture when compared to the uncirculated case. This is a result of the UHC and CO accumulation in the system as previously mentioned.

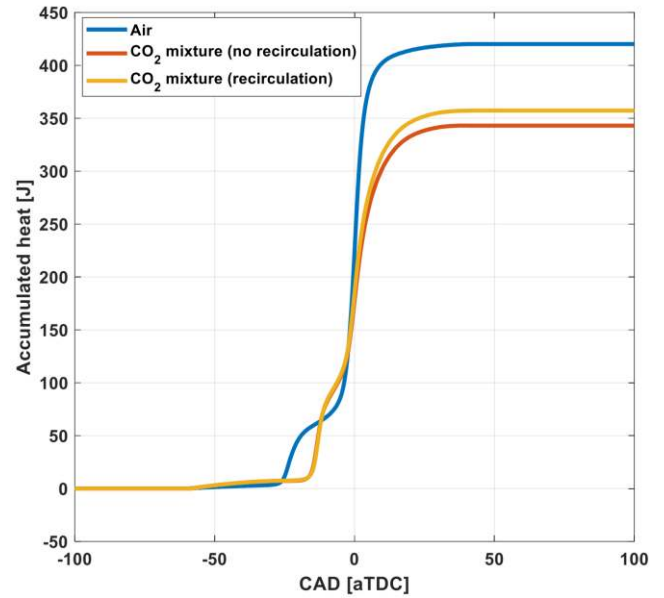The integration of the heat release rate gives the accumulated heat release shown in figure 9.

The combustion was phased such that 50% of heat is released just before TDC as seen in figure 9. It can be noticed that the LTHR of the CO_2 mixtures is higher than the LTHR of the air mixture. This is a direct result of the chemical effect of either fresh or recirculated CO_2 as previously discussed. Furthermore, the difference in the total heat release between the threes cases is a consequence of the CO_2 decreasing the system reactivity and consequently poor combustion efficiency η_c as shown later in the efficiency analysis.

Exhaust emissions

High unburned hydrocarbons (UHC) emissions are indicators for poor combustion efficiency. They are usually measured using a flame ionization detector (FID) that gives a reasonable measurement of the exhaust total hydrocarbons (THC). FTIR analyzer does not provide such THC reading but it measures a wide spectrum of hydrocarbons that are summed together to estimate the total hydrocarbons. While the FTIR is not as accurate as a conventional FID, it can still provide an acceptable UHC measurement. The following formula is used in this study to estimate UHC and it was also used by Melo et al. [33] for the same purpose.

$$UHC = CH_4 + 2C_2H_2 + 2C_2H_4 + 3C_3H_6 + 5IC_5 + 5NC_5 + 7.5AHC \qquad (9)$$

Where IC_5, NC_5, and AHC stand for iso-pentane, normal pentane, and total aromatics concentration, respectively.
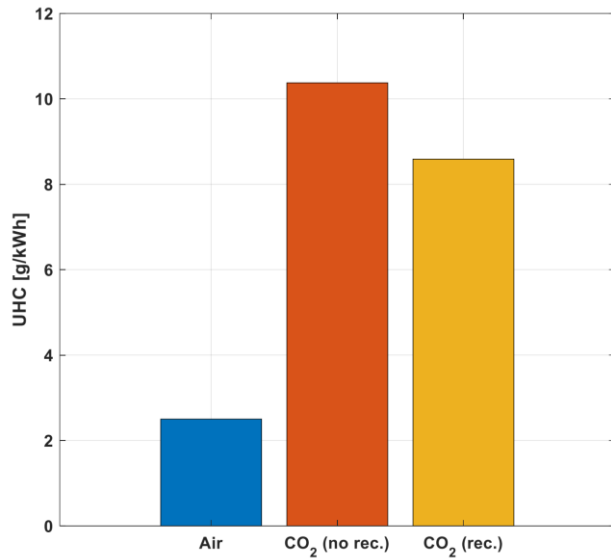
10/19/2016

Figure 10. Unburned hydrocarbon emissions for the three different mixtures

Figure 10 shows the unburned hydrocarbon (UHC) emissions for the three different mixtures. The least UHC emission level is observed for the air mixture as a result of the relatively high in-cylinder temperature. The reasons behind this high in-cylinder temperature was previously discussed in the *in-cylinder pressure and temperature* section. The high in-cylinder temperature assists the oxidation of the fuel and hence less unburned hydrocarbons are emitted. The uncirculated CO2 mixture showed slightly higher UHC emissions if compared to the recirculated case. This difference could be a result of the equivalence ratio disturbance in the case of the recirculated CO2 mixture. The recirculated gas will contain some traces of combustible gases that could enhance the combustion efficiency and result in less UHC. However, the difference is not much significant if compared to the air case.

Figure 11 shows the CO emissions for the three different mixtures. The recirculated CO2 mixture showed the highest CO emissions because of the CO traces in the recirculated exhaust. On the other hand, limited CO emissions can be observed in the case of air as a result of the relatively high in-cylinder temperature.
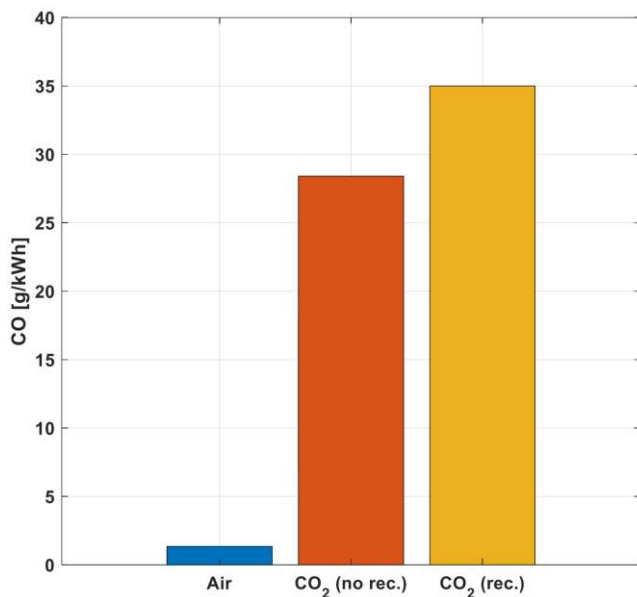

Figure 11. Carbon monoxide emissions for the three different mixtures

The main chemical mechanism driving the formation of NO_x in internal combustion engines is the Zeldovich mechanism [34]. NO_x formed by this mechanism are usually called thermal NO_x since high temperatures (>1700 K) are needed for the onset of the reactions. HCCI combustion is a low temperature combustion mechanism and the temperature needed for NO_x formation is not achieved. This justifies the low NO_x emissions shown in figure 12.
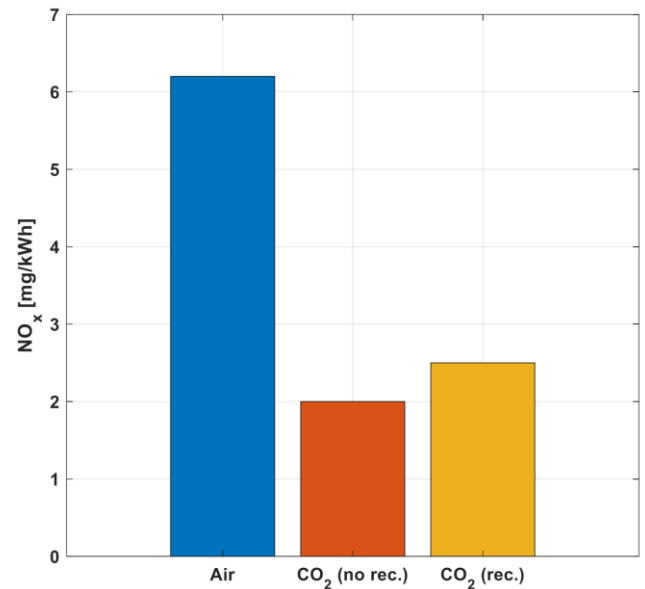

Figure 12. Nitrogen oxides emissions for the three different mixtures

Negligible NO_x emissions are observed in the case of the oxy-fuel combustion (CO_2 mixtures) although no nitrogen was supplied to the engine. This could be a result of the N_2 impurities in the O_2 and CO_2 cylinders.

Efficiency analysis

The scope of the present study covers three essential efficiencies contributing to the overall efficiency of the internal combustion engine. Those are the combustion efficiency η_c, the thermodynamic efficiency η_{th}, and the gas exchange efficiency η_{ge}. The product of the previous efficiencies is known as the gross indicated thermal efficiency η_{ind} as shown in equation 10.

$$\eta_{ind} = \eta_c \eta_{th} \eta_{ge} \qquad (10)$$

The details of the efficiency calculations is presented in the appendix of a paper previously published by the authors [35].

Combustion efficiency η_c

Combustion efficiency η_c determines the efficiency of converting the fuel chemical energy to thermal energy. The estimation of the combustion efficiency is based on analyzing the exhaust emissions and determining the amount of combustibles that could have been burned inside the cylinder but they were not. The main combustible species are unburned hydrocarbons (UHCs), carbon monoxide (CO), and hydrogen (H_2). The emissions are measured using an FTIR analyzer which cannot measure the concentration of H_2. In fact, FTIR cannot measure any diatomic molecule because of the lack of dipole moments that prevents the molecule from reacting to the IR radiation. Thus, hydrogen concentration was estimated using the water-gas equation assuming $K = 3.5$ [6] as shown in equation 11.

$$x_{H_2} = \frac{x_{CO} \, x_{H_2O}}{K \, x_{CO_2}} \qquad (11)$$

Where
x is the molar concentration of the associated molecule
K is the water-gas constant (assumed to be 3.5).

Those emissions are used to estimate the combustion efficiency η_c as per the following equation:

$$\eta_c = 1 - \frac{\Sigma \frac{M_i}{M_p} x_i Q_{LHV,i}}{\frac{1}{1 + \frac{A}{F}} Q_{LHV,f}} \qquad (12)$$

Where
M_i is the molar mass of species i (UHC, CO, H_2)
M_p is the molar mass of products
x_i is the mole fraction of species i (UHC, CO, H_2)
Q_{LHV} is the lower heating value of fuel f or species i
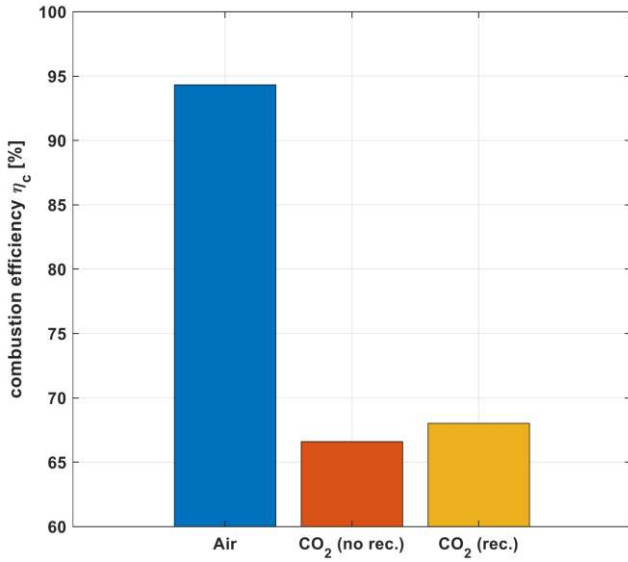A/F mass Air-fuel ratio (or CO_2 mixture-fuel ratio)

Figure 13. Combustion efficiency η_c for the three different mixtures

High in-cylinder temperature usually results in improved combustion efficiency since the elevated temperature assists the oxidation of the fuel. Figure 13 confirms that the air mixture, having the highest in-cylinder temperature, resulted in the maximum combustion efficiency. The decrease of the combustion efficiency η_c for the CO_2 mixtures is not only because of the high heat capacity of the CO_2 that decreases the in-cylinder temperature and consequently decreases the oxidation reactions. The chemical effect related to the possibility of CO_2 to directly participate in chemical reactions is also an important factor as previously mentioned. Again, the recirculation of the CO_2 mixture does not bring a significant difference as seen in figure 13.

Thermodynamic efficiency η_{th}

Thermodynamic efficiency determines how much of the thermal energy is converted to mechanical work on the piston. Since this process depends on the efficiency of expanding the hot gases in the cylinder, it is a function of the specific heat ratio that determines the evolution of pressure and temperature after combustion. Equation 13 shows the ideal thermodynamic efficiency which

depends on the compression ratio and the specific heat ratio of the mixture.

$$\eta_{th,ideal} = 1 - \frac{1}{R_c^{\gamma-1}} \qquad (13)$$

Where
$\eta_{th,ideal}$ is the ideal thermodynamic efficiency
R_c is the compression ratio
γ is the specific heat ratio

It should be noted that the real thermodynamic efficiency is lower than the ideal efficiency shown in equation 10 because the ideal efficiency neglects the heat transfer losses. Equation 10 can be rewritten if the following isentropic relation is used:

$$R_c = \frac{V_1}{V_2} = \left(\frac{T_2}{T_1}\right)^{\frac{1}{\gamma-1}} \qquad (14)$$

Where V is the volume, T is the temperature, and the subscripts 1 and 2 denote the property before and after compression, respectively.

Substituting (14) in (13), the thermodynamic efficiency can be written as:

$$\eta_{th} = 1 - \frac{T_1}{T_2} \qquad (15)$$

Equation 15 reveals that if two mixtures have the same initial temperature before compression and the same final temperature after compression then similar thermodynamic efficiency is expected. In this present study, all cases had the same temperature before compression and also the same temperature after compression. Thus, similar thermodynamic efficiency was observed as shown in figure 14. This can also be explained in light of equation 13. The air mixture has relatively higher γ but lower R_c while the CO_2 mixtures have the opposite with lower γ and higher R_c. The effect of one parameter cancels the effect of the other resulting in similar thermodynamic efficiency.
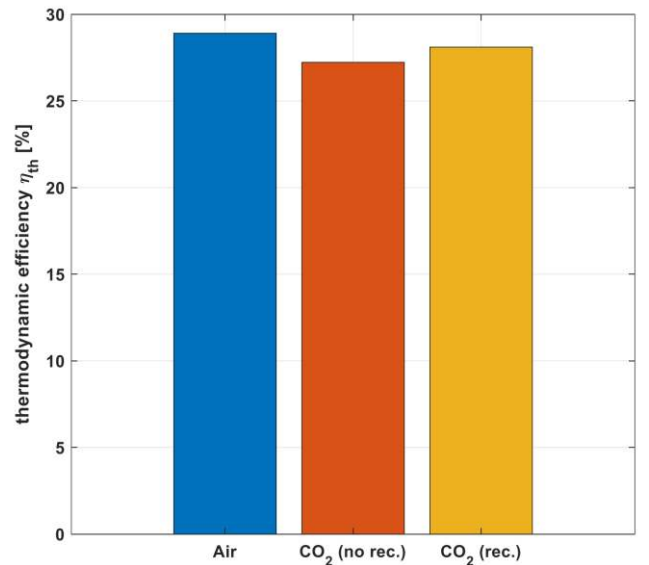

Figure 14. Thermodynamic efficiency η_{th} for the three different mixtures

10/19/2016

Gas exchange efficiency η_{ge}

Part of the energy released is utilized to push the burned gases out of the cylinder and pull in a fresh charge. The efficiency of this process is known as the gas exchange efficiency. In the case of the recirculated CO_2, the exhaust is throttled by a back pressure valve to increase the exhaust pressure and drive the EGR in the right direction. But increasing the exhaust pressure results in more lost pumping work to push the gases out of the cylinder. This explains why the recirculated CO_2 mixture is having the least gas exchange efficiency as shown in figure 15.
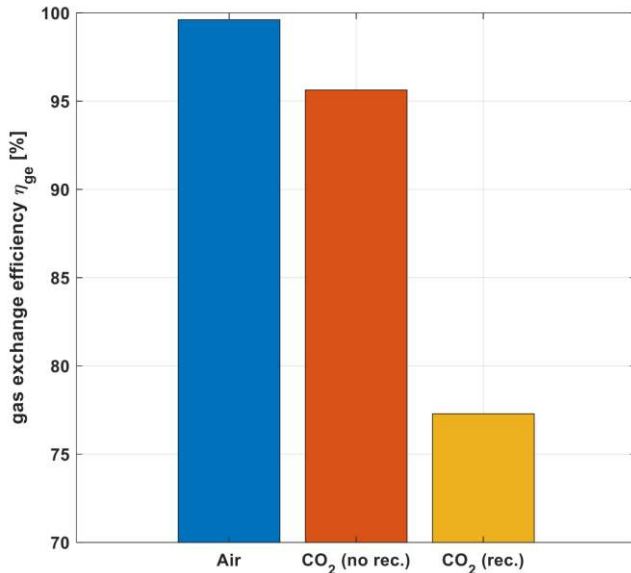

Figure 15. Gas exchange efficiency η_{ge} for the three different mixtures

One more observation in figure 15 is that the uncirculated CO_2 mixture has less gas exchange efficiency than the air mixture. This is a result of the CO_2 mixture being heavier than air and thus requiring more pumping work.
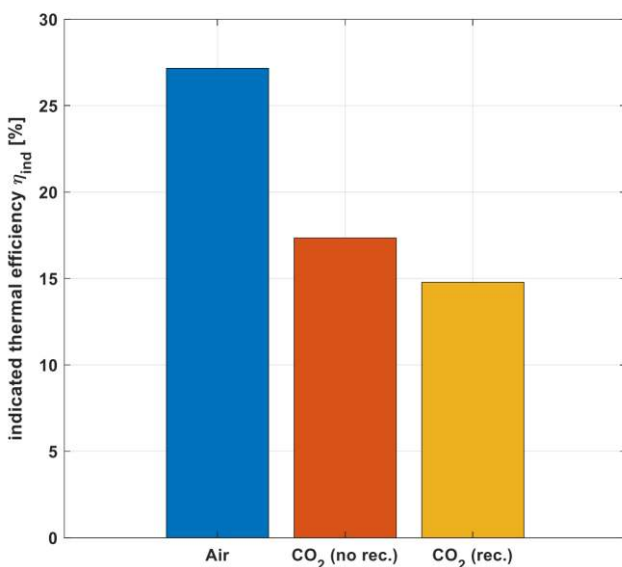
Gross indicated thermal efficiency $\eta_{ind,th}$

Figure 16. Indicated thermal efficiency η_{ind} for the three different mixtures

Figure 16 shows the indicated thermal efficiency for the three different cases. The air mixture resulted in the highest indicated thermal efficiency because of the higher in-cylinder temperature that gives better combustion efficiency and the lighter mixture that results in less pumping losses. The main difference between the uncirculated CO_2 mixture (case 2) and the recirculated oxy-fuel combustion (case 3) was in the gas exchange efficiency. The EGR required higher exhaust pressure which required more pumping work and hence lower gas exchange efficiency. Figure 17 summarizes all the efficiency results.
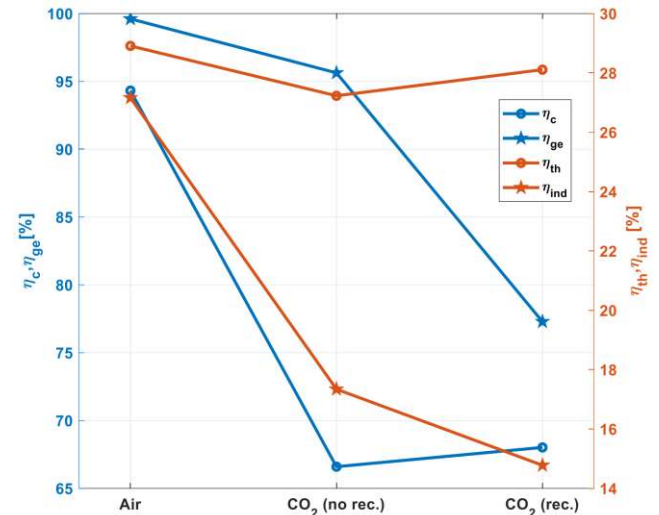

Figure 17. Summary of the efficiency results

Conclusion

The present study investigated the oxy-combustion of a carbon fuel in an ICE with dry EGR. Single cylinder variable compression ratio CFR engine modified to run in HCCI conditions was used for the experiments. Three different cases were studied: normal combustion with air as the oxidizer, oxy-fuel combustion without EGR, and oxy-fuel combustion with dry EGR. The relatively reactive n-heptane was used as the fuel because CO_2 decreases the in-cylinder temperature and combustion would not be possible if less reactive fuels are used. The combustion was phased by adjusting the compression ratio to have CA50 at TDC for all three cases. In-cylinder pressure was measured and the temperature was derived from the pressure trace using the ideal gas low. Pressure trace is also used to estimate the charge specific heat ratio (γ), heat release rate (HRR), thermodynamic efficiency (η_{th}), and gas exchange efficiency (η_{ge}). Combustion efficiency (η_c) was derived from the emissions measured by the FTIR analyzer. The results showed that HCCI oxy-fuel combustion with recirculated exhaust gases is possible. Possibility does not mean practicality, in fact, there are many issues to be addressed before such a concept can exist in markets. Oxygen separation, the relatively low combustion and thermodynamic efficiencies, and the low gas exchange efficiency because of the EGR are some of those issues. Future studies may crank up the compression ratio and use better engine geometry to enhance the overall engine efficiency. Running the engine at more practical speeds that are not possible with the CFR could also be a pathway for better understanding and evaluation of this concept. The following list summarizes the conclusions of the study:

1. Operating an HCCI engine with a mixture of oxygen and carbon dioxide instead of air gives pure CO_2 in the exhaust. This can be used for carbon capture technologies.

2. Using recirculated CO_2 from the exhaust instead of pure CO_2 from bottles could matter as real exhaust contains NOx, CO and unburned hydrocarbons. However, small differences between real exhaust CO_2 and synthetic could be observed.
3. The results in terms of emissions and thermodynamic efficiency were all the same for pure CO_2 and recirculated CO_2 (EGR).
4. The gas exchange efficiency was lower with real exhaust CO_2 but this could be due to engine operating conditions with higher exhaust back pressure to drive the EGR.
5. The engine efficiency with oxygen and CO_2 is very low. The net indicated efficiency is only 18% with pure CO2 and it drops further to 15% with recirculated CO_2.
6. To reach auto ignition temperature, very high compression ratio is needed and even then, a very reactive fuel like n-heptane must be selected. The high compression ratio does not give high thermodynamic efficiency as the gamma is low for CO_2.
7. Overall, using HCCI with oxygen and recirculated CO_2 cannot be recommended for carbon capture systems.

References

1. Wright, L.D., Syvitski, J.P.M., and Nichols, C.R., "Global Change: More Than Climate," in: Wright, L. D. and Nichols, C. R., eds., *Tomorrow's Coasts: Complex and Impermanent*, Springer International Publishing, Cham, ISBN 978-3-319-75453-6: 25–46, 2019, doi:10.1007/978-3-319-75453-6_2.
2. Forster, P., "Half a century of robust climate models," *Nature* 545:296, 2017.
3. Wuebbles, D.J., Fahey, D.W., Hibbard, K.A., Dokken, D.J., Stewart, B.C., and Maycock, T.K., "Climate Science Special Report: Fourth National Climate Assessment, Volume I," Washigton, DC, USA, 2017, doi:10.7930/J0J964J6.
4. Metz, B., Davidson, O.R., Bosch, P.R., Dave, R., and Meyer, L.A., "Climate Change 2007: Mitigation. Contribution of Working Group III to the Fourth Assessment Report of the Intergovernmental Panel on Climate Change," New York, USA, 2007.
5. Joshi, A., Review of Vehicle Engine Efficiency and Emissions, 2019, doi:https://doi.org/10.4271/2019-01-0314.
6. Johansson, B. and universitet. Institutionen för energivetenskaper, L., "Combustion Engines," Department of Energy Sciences, Lund University, ISBN 9789176230954, 2014.
7. Elgowainy, A., Han, J., Ward, J., Joseck, F., Gohlke, D., Lindauer, A., Ramsden, T., Biddy, M., Alexander, M., Barnhart, S., Sutherland, I., Verduzco, L., and Wallington, T.J., "Current and Future United States Light-Duty Vehicle Pathways: Cradle-to-Grave Lifecycle Greenhouse Gas Emissions and Economic Assessment," *Environ. Sci. Technol.* 52(4):2392–2399, 2018, doi:10.1021/acs.est.7b06006.
8. Sharma, T.K., Rao, G.A.P., and Murthy, K.M., "Homogeneous Charge Compression Ignition (HCCI) Engines: A Review," *Arch. Comput. Methods Eng.* 23(4):623–657, 2016, doi:10.1007/s11831-015-9153-0.
9. Hyvönen, J., Haraldsson, G., and Johansson, B., "Operating range in a Multi Cylinder HCCI engine using Variable Compression Ratio," *2003 JSAE/SAE International Spring Fuels and Lubricants Meeting*, SAE International, 2003, doi:https://doi.org/10.4271/2003-01-1829.
10. Najafabadi, M.I. and Aziz, N.A., "Homogeneous Charge Compression Ignition Combustion : Challenges and Proposed Solutions," *J. Combust.* 2013:14, 2013, doi:https://doi.org/10.1155/2013/783789.
11. Bilgin, B., Magne, P., Malysz, P., Yang, Y., Pantelic, V., Preindl, M., Korobkine, A., Jiang, W., Lawford, M., and Emadi, A., "Making the Case for Electrified Transportation," *IEEE Trans. Transp. Electrif.* 1(1):4–17, 2015, doi:10.1109/TTE.2015.2437338.
12. Kawamoto, R., Mochizuki, H., Moriguchi, Y., Nakano, T., Motohashi, M., Sakai, Y., and Inaba, A., "Estimation of CO2 Emissions of Internal Combustion Engine Vehicle and Battery Electric Vehicle Using LCA," *Sustainability* 11(9), 2019, doi:10.3390/su11092690.
13. Buhre, B.J.P., Elliott, L.K., Sheng, C.D., Gupta, R.P., and Wall, T.F., "Oxy-fuel combustion technology for coal-fired power generation," *Prog. Energy Combust. Sci.* 31(4):283–307, 2005, doi:https://doi.org/10.1016/j.pecs.2005.07.001.
14. Bilger, R.W. and Wu, Z., "Carbon Capture for Automobiles Using Internal Combustion Rankine Cycle Engines," *J. Eng. Gas Turbines Power* 131(3), 2009, doi:10.1115/1.3077657.
15. Hashim, S.S., Mohamed, A.R., and Bhatia, S., "Oxygen separation from air using ceramic-based membrane technology for sustainable fuel production and power generation," *Renew. Sustain. Energy Rev.* 15(2):1284–1293, 2011, doi:https://doi.org/10.1016/j.rser.2010.10.002.
16. Boer, P.C.T. de and Hulet, J.F., "Performance of a hydrogen-oxygen-noble gas engine," *Int. J. Hydrogen Energy* 5(4):439–452, 1980, doi:10.1016/0360-3199(80)90024-5.
17. Bilger, R.W., "Zero release combustion technologies and the oxygen economy," *Fifth International Conference on Technologies and Combustion for a Clean Environment, Lisbon, Portugal, Jul*, 12–15, 1999.
18. Wu, Z.-J., Yu, X., Fu, L.-Z., Deng, J., Hu, Z.-J., and Li L.-G., "A high efficiency oxyfuel internal combustion engine cycle with water direct injection for waste heat recovery," *Energy* 70:110–120, 2014, doi:https://doi.org/10.1016/j.energy.2014.03.095.
19. Fu, L., Wu, Z., Yu, X., Deng, J., Hu, Z., and Li, L., "Experimental Investigation of Combustion and Emission Characteristics for Internal Combustion Rankine Cycle Engine under Different Water Injection Laws," *Energy Procedia* 66:89–92, 2015, doi:https://doi.org/10.1016/j.egypro.2015.02.047.
20. Yu, X. and Wu, Z.J., "Simulation on Effect of EGR on Oxy-Fuel IC Engine," *Mechanical and Electronics Engineering III*, Trans Tech Publications Ltd: 790–795, 2012, doi:10.4028/www.scientific.net/AMM.130-134.790.
21. Boretti, A., Osman, A., and Aris, I., "Direct injection of hydrogen, oxygen and water in a novel two stroke engine," *Int. J. Hydrogen Energy* 36(16):10100–10106, 2011, doi:https://doi.org/10.1016/j.ijhydene.2011.05.033.
22. Osman, A., "Feasibility Study of a Novel Combustion Cycle Involving Oxygen and Water," *SAE 2009 Powertrains Fuels and Lubricants Meeting*, SAE International, 2009, doi:https://doi.org/10.4271/2009-01-2808.
23. Kang, Z., Wu, Z., Zhang, Z., Deng, J., Hu, Z., and Li, L., Study of the Combustion Characteristics of a HCCI Engine Coupled with Oxy-Fuel Combustion Mode, 2017, doi:https://doi.org/10.4271/2017-01-0649.
24. Mohammed, A., MASURIER, J.-B., Elkhazraji, A., and Johansson, B., "Oxy-Fuel HCCI Combustion in a CFR Engine with Carbon Dioxide as a Thermal Buffer," *14th International Conference on Engines & Vehicles*, SAE International, 2019, doi:https://doi.org/10.4271/2019-24-

0119.

25. Brock, C. and Stanley, D.L., "The Cooperative Fuels Research Engine : Applications for Education and Research," 1:130–135, 2012, doi:10.5703/1288284314865.

26. ASTM, "Standard Test Method for Motor Octane Number of Spark-Ignition Engine Fuel 1," *Annu. B. ASTM Stand.* (C):1–56, 2011, doi:10.1520/D2700-11.2.

27. Burcat, A., "Third Millennium Ideal Gas and Condensed Phase Thermochemical Database for Combustion with Updates from Active Thermochemical Tables," (September), 2005.

28. Scaringe, R.J., "Extension of the high load limit in the Homogeneous Charge Compression Ignition engine," *PhD Dissertation*, Massachusetts Institute of Technology, 2009.

29. Singh, E., Waqas, M., Johansson, B., and Sarathy, M., "Simulating HCCI Blending Octane Number of Primary Reference Fuel with Ethanol," (Ci), 2017, doi:10.4271/2017-01-0734.

30. Gatowski, J.A., Balles, E.N., Chun, K.M., Nelson, F.E., Ekchian, J.A., and Heywood, J.B., "Heat Release Analysis of Engine Pressure Data," *1984 SAE International Fall Fuels and Lubricants Meeting and Exhibition*, SAE International, 1984, doi:https://doi.org/10.4271/841359.

31. Woschni, G., "A Universally Applicable Equation for the Instantaneous Heat Transfer Coefficient in the Internal Combustion Engine," *National Fuels and Lubricants, Powerplants, Transportation Meetings*, SAE International, 1967, doi:https://doi.org/10.4271/670931.

32. Sabia, P., Lubrano, M., Giudicianni, P., Sorrentino, G., and Ragucci, R., "CO 2 and H 2 O effect on propane auto-ignition delay times under mild combustion operative conditions," *Combust. Flame* 162(3):533–543, 2015, doi:10.1016/j.combustflame.2014.08.009.

33. Melo, T.C.C. De, MacHado, G.B., Belchior, C.R.P., Colaço, M.J., Barros, J.E.M., Oliveira, E.J. De, and Oliveira, D.G. De, "Hydrous ethanol-gasoline blends - Combustion and emission investigations on a Flex-Fuel engine," *Fuel* 97:796–804, 2012, doi:10.1016/j.fuel.2012.03.018.

34. Warnatz, J., Maas, U., Dibble, R.W., and Dibble, R.W., "Combustion: Physical and Chemical Fundamentals, Modelling and Simulation, Experiments, Pollutant Formation.," Springer, ISBN 9783540677512, 2001.

35. Mohammed, A.M., Masurier, J.-B., Elkhazraji, A., Dibble, R., and Johansson, B., "A path towards high efficiency using Argon in an HCCI engine," *WCX SAE World Congress Experience*, SAE International, 2019.

Contact Information

Abdulrahman Magdy Mohammed – PhD student
King Abdullah University of Science and Technology
Clean Combustion Research Center, IC Engines Laboratory,
Alkindi Building Sea Side (Building 5), 4203-WS19
M +966 530264193
P.O. Box 4700 KAUST Thuwal, JEDDAH 23955
abdulrahman.mohammed@kaust.edu.sa

Acknowledgements

Abbreviations

BEV	**Battery electric vehicle**
CA50	**Crank angle degree at which 50% of heat is already released**
CFR engine	**Cooperative fuel research engine**
EGR	**Exhaust gas recirculation**
FID	**Flame ionization detector**
FTIR	**Fourier transform infra-red**
GHG	**Greenhouse gases**
HCCI	**Homogenous charge compression ignition**
HR	**Heat release**
HRR	**Heat release rate**
ICE	**Internal combustion engine**
ICRC	**Internal combustion Rankine cycle**
LTHR	**Low temperature heat release**
MFC	**Mass flow controller**
MON	**Motor octane number**
RON	**Research octane number**
SI	**Spark ignition**
TDC	**Top dead center**
THC	**Total hydrocarbons**
UHC	**Unburned hydrocarbons**
USGCRP	**U.S. Global Change Research Program**

10/19/2016

10/19/2016